Tutor/s

Dr. Fermín Huarte Larrañaga
Departament de Ciència de materials i Química Física

Dr. Pablo Gamallo Belmonte
Departament de Ciència de materials i Química Física

Grau de Química

Treball Final de Grau

Carbon based membranes as filtering materials for gaseous mixtures.

Membranes de base carbònica per al filtratge selectiu de mescles gasoses.

Jesús Antón Quílez

June 2021

Universitat de Barcelona

B:KC Barcelona Knowledge Campus
Campus d'Excel·lència Internacional

Sigues un químic físic, un químic analític, un químic orgànic, si ho vols; però per sobre de tot, sigues un químic.

Ira Remsen

Vull agrair a en Fermín i a en Pablo pel seu suport i per tot el que m'han ensenyat durant la realització del projecte, així com als professors que m'han format durant aquests anys i els amics que he fet a la universitat. També vull agrair a la meva mare, al meu avi, a les meves germanes i a la meva parella per recolzar-me durant tot aquest temps i encara més durant aquesta temporada difícil.

REPORT

CONTENTS

1. SUMMARY

Carbon-based membranes are a novel approach to gas separation. More precisely, new graphene-like structures are of utmost importance in this field of research. The scope of this work is to prove the effectiveness of grazyne membranes in the separation of different gaseous mixtures: carbon dioxide (CO_2) with methane (CH_4) and CO_2 with oxygen (O_2). To determine the efficiency of the membrane, a molecular dynamics simulation is carried via Large-scale Atomic/Molecular Massively Parallel Simulator (LAMMPS) undergoing an adaptive intermolecular reactive bond order (AIREBO) force field.

Grazynes are a recently proposed family of 2D carbon allotropes consisting in graphene-like stripes bonded via acetylenic links, which allow for the design of pores of variable size, an important property for gas separation. For these simulations, the studied membrane was [1],[2]{2}-grazyne. The focus of the research was to determine their permeability and selectivity for both mixtures at different sets of pressures and constant temperature. To achieve this, a box was simulated in which a piston-like wall was set at different heights. Due to computational restraints, simulations at low pressure values (i.e. lower than 10 atm) were performed with c(2x2) supercells. The results were conclusive in determining the [1],[2]{2}-grazyne membrane as infinitely selective for CO_2 over CH_4 between 1 and 20 atm, meaning the membrane was impermeable for methane.

For the CO_2/O_2 mixture, further simulations were performed with [1],[3]- and [1],[m]{1}-grazynes (m=1,2,3) as no selective separation could be carried out. No conclusive data could be obtained from such simulations, as the only selective separations occurred when only a single molecule was filtered.

Keywords: Grazynes, Gas separation, Carbon-based membranes, CO_2, CH_4, O_2, Selectivity, Permeability, Permeance, LAMMPS, AIREBO.

2. RESUM

Les membranes basades en el carboni són un nou mètode per la separació de gasos. Més precisament, les estructures ressemblant el grafè son algunes de les més importants per aquest camp de la ciència. L'abast d'aquest projecte és demostrar l'eficiència de les membranes de grazí per la separació de mescles de diferents gasos: diòxid de carboni (CO_2) amb metà (CH_4) i CO_2 amb oxigen (O_2). Per determinar l'eficàcia de la membrana, les simulacions de dinàmica molecular es van realitzar mitjançant el Simulador en Paral·lel Massiu Atòmic/Molecular de Llarg abast (LAMMPS, en anglès) sota un camp de forces d'Ordre d'Enllaç Reactiu Adaptatiu Intermolecular (AIREBO, en anglès).

Els grazins són una família d'al·lòtrops del carboni en 2D recentment proposada que consisteixen en fileres semblants a les del grafè unides per enllaços acetilènics, que permeten el disseny de porus de mida variable, una propietat important per la separació de gasos. Per aquestes simulacions, la membrana estudiada va ser el [1],[2]{2}-grazí. L'objectiu d'aquest projecte va ser determinar la seva permeabilitat i selectivitat per ambdues mescles a diferents rangs de pressions i temperatura constant. Per aconseguir-ho, es va simular una caixa on una paret semblant a un pistó se situava a diferents alçades. Per culpa de limitacions computacionals, les simulacions a valors baixos de pressions (inferiors a 10 atm) es van realitzar amb supercel·les c(2x2). Els resultats van ser conclusius al determinar que la membrana de [1],[2]{2}-grazí era infinitament selectiva pel CO_2 sobre el CH_4 entre 1 i 20 atm, el que vol dir que es considera impermeable pel metà.

Per la mescla de CO_2/O_2, es van realitzar més simulacions amb les membranes de [1],[3]- i [1],[m]{1}-grazins (m=1,2,3) ja que no es va poder realitzar una separació selectiva. No es va poder obtenir cap informació concloent de les simulacions, ja que les úniques separacions selectives es van dur a terme en casos on només es filtrava una molècula.

Paraules clau: Grazins, Separació de gasos, Membranes basades en el carboni, CO_2, CH_4, O_2, Selectivitat, Permeabilitat, Permeància, LAMMPS, AIREBO.

3. INTRODUCTION

Separation of gaseous mixtures has been a subject of research in industry for many years. The isolation of harmful products such as methane or carbon dioxide to reduce widespread pollution or the recovery and recirculation of components presents in waste gases to reduce costs are some of the reasons why this area is important.

Moreover, the United Nations (UN) stated in its 9th goal of the 2030 Agenda for Sustainable Development the need of a more sustainable industrialization. Which means that a way to reduce atmospheric contamination must be developed to work towards fixing the many issues with current production-based pollution.[1] The separation and isolation of components in gaseous mixtures can lead to an increase in pollution control due to its theoretical high selectivity.

Gas separation via membranes is widely performed to separate various components of gaseous mixtures. Whether using polymeric, nanoporous or carbon-based membranes, it is a staple method for an effective separation, providing energy efficient solutions and high rates for both permeability and separation. Membrane separation is a flowering market which has been replacing traditional separation methods in both industry and research fields.[2]

Grazyne membranes might be a new important field of research due to the many different structures which can be obtained by modifying the number of graphene-like units, length of acetylenic bonds or its removal. The different pore areas lead to varying performance for gas separation, meaning a commercial grazyne layer could effectively be impermeable for CH_4 while permeating smaller gaseous molecules, which could be interesting for storing the methane present in sewer gases. Another membrane could be commercialized being impermeable to CO_2, which could be placed on hospital windows in areas where patients have lung issues.

The possibilities for gas separation via grazyne membranes seem unending because of its ease of design and being a graphene derivate, meaning that grazyne keeps many of its already revered properties.

4. OBJECTIVES

The overall framework of this research is the general design of grazynic membranes, selecting candidates that are capable of separating a gaseous mixture of choice. More specifically, we have employed computational tools to carry out a detailed simulation via LAMMPS of the selectivity and permeability of the [1],[2]{2}-grazyne membrane for two gaseous mixtures: CH_4 with CO_2 and O_2 with CO_2. For this, different parameters concerning the simulation: such as the box's size limits, temperature and running time must be defined. For the molecules, values for their spatial arrangements, interactions and potentials must be established before running the simulation. The objectives of this project are the following:

- Choosing and designing two membrane candidates for the separation of CO_2/CH_4 and CO_2/O_2 mixtures.
- Determining the selectivity of each mixture through the obtained trajectory results from several Molecular Dynamics simulations at a pressure range and constant temperature under a force field.
- Determining the permeability and permeance of the various mixtures under the initial and new conditions.
- Concluding if any of the proposed membranes is a selective separation method for any of the components in the mixtures.

5. THEORY

5.1 MOLECULAR DYNAMICS

Molecular Dynamics is a powerful computer simulation tool, frequently used to model time-dependent properties on a many-body system without taking quantum effects into consideration, which means the simulation only follows the laws of classical mechanics.[3] Molecular Dynamics (MD) provide great improvements against prior computer-simulated techniques, being an alternative to the previous Monte Carlo (MC) method in areas where MC couldn't perform calculations. Some of these advantages, besides managing to perform time-dependent calculations, are being able to work in parallel with each atom of the system, while MC is only able to move one particle at a time, and calculating torsional effects in large molecules, which is highly cost-intensive for MC simulations.

The process of MD simulations can be summarized in a loop consisting of three parts: the calculation of forces, the integration of the equations of motion and the averaging of the system properties.

Before starting the loop, the program reads the initialization parameters, which contain information regarding the system's conditions, such as the initial temperature or the starting coordinates of the particles. These parameters are introduced before the loop because they are the initial state of the system and are supposed to change in time, i.e. the particles' velocities, which are computed from a random number and a set temperature, or the molecules' coordinates, which will move during time. Some other parameters are set to be invariable, which is the case of temperature or pressure. This is obtained via ensembles, which are an aggrupation of particles under the same fixed conditions. In the case of this work, simulations were done under the NVT ensemble, meaning that the number of atoms (N), the volume (V) and the temperature (T) where fixed. Volume can be set in a fixed position by creating a piston-like wall, which combined by the invariable temperature allows to work at a fixed pressure in one side of the membrane while creating a pressure gradient to facilitate diffusion. This is an advantage over the NPT ensemble.

Besides the simulation parameters, more data needs to be input when considering the initialization of the system. Coordinates don't provide enough information about connectivity and topologic information needs to be supplied. Chemical bonds, angles and dihedrals must be defined between atoms along with their equilibrium length (or angle) and energies.

Due to the system being simulated inside a theoretical box (see the Results section for a diagram of the box), there are so called periodic boundary conditions (PBC) that aim to reduce possible boundary effects caused by the size of the box. In the case of this research, there would be no side walls, meaning that a molecule reaching one side would exit through the other, instead of colliding with a wall, but there would be lower and upper walls because the number of molecules at each side of the membrane mattered. To ease the computational process, all the parameters concerning an ensemble can be confined in the lattice of the membrane's unit cell (in this case) and then the cell can be replicated as a matrix.

After the initialization of the system the fulfillment of the main loop (which will be explained in detail in the following sections) consists of obtaining numerical solutions of the equations of motion for every timestep. To do so, the resulting force is computed as a derivative of an obtained potential energy and its interaction with neighbor particles. The potential for these non-bonding interactions could be expressed as sum of many bodies, but to avoid computational constraints, are normally limited only to pairs.[4]

For the last step of the loop, boundary conditions are applied. This is an important step because it is not unusual to have the simulation stopped because a particle is out of bounds, normally because the length of the timestep is too large. Other parameters controlled are pressure and temperature, which are updated for every timestep and usually written in an output file to allow for compliance with the obtained trajectories. Besides pressure and temperature data, the simulation can perform calculations for total, kinetic and potential energy and output them for each timestep. After this process, the timestep is increased and the loop is repeated.

5.1.1 Equations of Motion

MD simulations are based on the integration of Newton's second law, also known as the equation of motion (Eq. 1) and usually the software solves them for each atom and step of the simulation.

$$F_i = m_i a_i = m_i \frac{d^2 r_i}{dt^2} \qquad \text{(Eq. 1)}$$

Where m_i is the mass of a given particle and r_i is a vector containing the coordinates of a particle in all three axes. a_i is the acceleration in all three coordinates of a particle, here defined as the second derivate of position over time.

Force can also be represented as the derivate of the potential energy of the system, which can be easily obtained through the force field parameters, with respect to the position of a particle. Which would result in Eq. 2, Where V is the potential energy of the system.

$$-\frac{dV}{dr_i} = m_i \frac{d^2 r_i}{dt^2} \qquad \text{(Eq. 2)}$$

Knowing the force applied over any particle allows to determine the particle's acceleration, but also its velocity and position as they ultimately are derivates of acceleration respect time. By integrating the acceleration, the classical approach to position calculation can be expressed (Eq. 3).

$$r(t) = \frac{1}{2}at^2 + v_o t + r_0 \qquad \text{(Eq. 3)}$$

Eq. 3 means that to obtain the coordinates of a particle in a time t, the only needed parameters are the acceleration (obtained from the system's potential energy), the initial distribution of velocities and the initial coordinates (obtained from the data file).

This method, however, needs the distribution of velocities, where the velocities in each direction is obtained from a Maxwell-Boltzmann distribution at a certain temperature. This, in turn, means the temperature needs to be computed for all atoms of the system from the velocities, and it must be solved numerically, which comes at a great cost. Computers can perform numerical approaches with significative accuracy using algorithms that resemble the classical equations of motion while being less cost intensive.

5.1.1.1 Verlet Algorithm

One of the most popular algorithms is the Verlet one, excelling in simplicity while offering great accuracy for the calculation of positions, but not so great for velocities. The Verlet algorithm updates the information of position (next timestep) performing a Taylor series expansion over present data of position, velocity, and acceleration (calculated as F/m), see Eq. 4 for the final expression of the Verlet Algorithm used, approximated to a simpler equation which doesn't lose much accuracy.

$$r(t + \Delta t) \approx 2r(t) - r(t - \Delta t) + \frac{F(t)}{m}\Delta t^2 \qquad \text{(Eq. 4)}$$

Where Δt is the timestep, r is the position of the particle, F is the applied force over the particle and m is the mass. The error for this expression is of the order $\mathcal{O}(\Delta t^4)$, which is acceptable as a low-cost integration tool.

From this final equation it is seen that the only necessary parameters to obtain the new coordinates at the next timestep ($t + \Delta t$) are the coordinates and applied force (obtainable from the potential energy) at the current timestep (t) and the coordinates of the previous timestep ($t - \Delta t$). This algorithm spares the cost of determining the velocities and doesn't need to perform many calculations, as the coordinates for (t and t-Δt) are already stored from the previous iteration. After the calculations of the current equation, the stored data is updated with the new one, in order to unload the memory from unnecessary information.

The Verlet algorithm is a great low-cost method for computing the trajectory of the particles in systems with many bodies, but its accuracy decreases greatly when determining the velocities. The velocity can be derived from the position equation but is a rarely used expression because the accuracy decreases considerably and needs information for positions at the next timestep, which would mean storing extra data for obtaining energetic and thermodynamic properties. For this reason, the Velocity Verlet[5] algorithm is preferred. See Eq. 5.

$$v(t + \Delta t) = v(t) + \frac{1}{2m}\big(F(t) + F(t + \Delta t)\big)\Delta t \qquad \text{(Eq. 5)}$$

The error for this algorithm is of order $\mathcal{O}(\Delta t^2)$, but the computational cost of this method is lower, and is considered a better approach than the previous Verlet derivate.

5.1.1.2 Other Algorithms

There are different alternatives to the Verlet algorithm when simulating many-bodies systems, depending on the simulation, every different approach comes with computational benefits and costs. One of the more widely used is the Leap-frog algorithm, which receives that name because the velocities are calculated for a time t+Δt/2 using the positions at time t, and then the positions calculation at time t+Δt leap over the velocities calculated at half the timestep. See Figure 1 for a diagram of the difference between both algorithms.

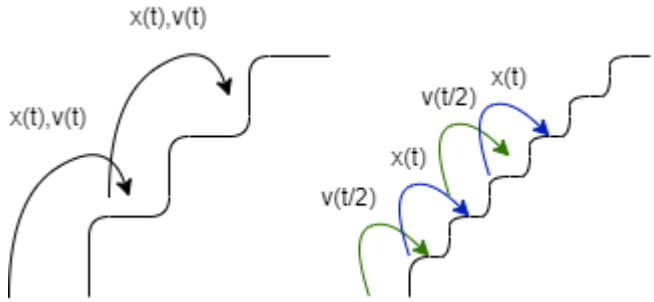

Figure 1. Difference in the calculation steps of Verlet (left) and Leap-frog (right) algorithms.

The other alternative to the Verlet algorithm is the Beeman one, which is able to calculate positions and velocities which greater accuracy but coming at the expense of being more cost intensive. Ultimately, Verlet is the preferred method because of its simplicity and acceptable accuracy without sacrificing resources.

5.2 FORCE FIELDS

In Molecular Dynamics, the correct description of the forces taking part in the simulation is of most importance. Force fields are used as a technique to determine intramolecular and intermolecular forces and its evolution during time. These fields use a set of equations and parameters to describe the potential energy of the studied system. The system's equations can be split into two terms: bonding energy, for contributions due to covalent bond, and non-bonding energy, to describe electrostatic, repulsive or Van der Waals interactions; both of these terms can be further broken down depending on the force field. The functions used to represent a system can vary in terms of complexity, where equations are more complex the more particular the studied phenomena are. This affects simulation times, as more accurate results translate into a higher computational resource cost.[6]

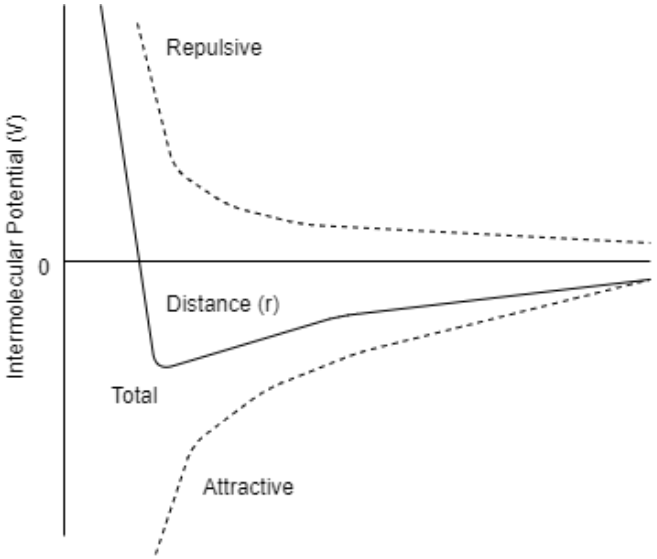

Figure 2. Intermolecular potential for any system of two interacting particles.

5.2.1 REBO

To overcome the limitations of classical molecular simulations (i.e. inability to modify bonds) and to attain non-intensive computational calculations of systems containing large numbers of atoms, the reactive empirical bond order (REBO) model was proposed. This model consists in the definition of an empirical interatomic potential providing the total energy of the system as a function of the system's particle coordinates.[7] REBO models normally define the potential as a contribution of both attractive and repulsive ones (Eq. 6):

$$E = \sum_i \sum_{i<j} \left[V_r(r_{ij}) + \overline{b_{ij}} V_A(r_{ij}) \right] \qquad \text{(Eq. 6)}$$

Where V_r is the term concerning core-core repulsive interactions, V_A are attractive interactions caused by valence electrons and b_{ij} is a decreasing function which weighs the number, strength, and angles of the competing bonds.

This model does not come without drawbacks, as its results lose accuracy when compared with ab-initio calculations due to the lack of more detailed interactions such as intermolecular, long range or torsional ones. Systems containing large hydrocarbons are some of the most affected, as intermolecular interactions are of great importance to study those systems. For these reasons, the adaptive intermolecular REBO (AIREBO) model was introduced. This function overcomes the previous REBO limitations, as it is effective for interactions in systems containing large hydrocarbons (such as graphites) while allowing for chemical reactions.[8]

5.2.2 AIREBO

AIREBO potentials are represented by the sum of a system's pairwise interactions, which consist in the REBO and torsion interactions and the Lennard-Jones (LJ) terms (Eq. 7):

$$E = \frac{1}{2} \sum_i \sum_{j \neq i} \left[E_{ij}^{REBO} + E_{ij}^{LJ} + \sum_{k \neq i,j} \sum_{l \neq i,j,k} E_{kijl}^{tors} \right] \qquad \text{(Eq. 7)}$$

Where the Lennard-Jones potential is included because it is one of the most robust and documented models for studying pairwise interactions thanks to its simplicity and affordable ease to compute:

$$V = 4\epsilon \left\{ \left(\frac{\sigma}{r} \right)^{12} - \left(\frac{\sigma}{r} \right)^{6} \right\} \qquad \text{(Eq. 8)}$$

This model (Eq. 8) consists of a contribution based on dispersion forces (London), which are considered attractive and proportional to $1/r^6$, and a repulsive contribution defined as proportional to $1/r^{12}$ which has a stronger influence at short distances between the particles (hence the repulsive contribution), where r is the distance between both interacting particles.

The rest of the parameters are ϵ, which is the depth of the potential well (determines the strength of the attraction) and σ is the separation at which the pairwise potential equals zero, it is also known as the van der Waals radius.

It is to be noted that the $1/r^{12}$ approximation is not an accurate way of representing the repulsive interaction, the exponential function $e^{-r/\sigma}$ is more accurate as a model of the distance dependence of repulsive forces.[9] Even so, the (12,6) potential provides an accurate enough potential when combined with the rest of AIREBO terms and offers the cost-effective solution of only calculating the r^6 term, as r^{12} is just the square of it. Whilst the most accurate solution involves calculating via an exponential function for every pairwise interaction for every step of the simulation, which would be very cost intensive. See Figure 3 for an illustration of the LJ potential and its attractive and repulsive components.

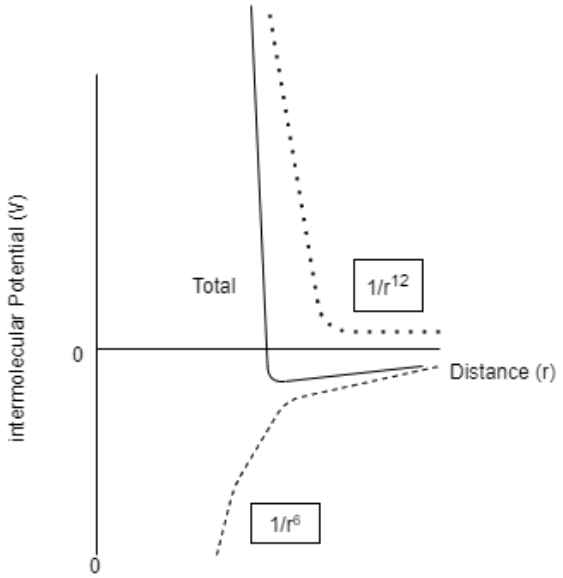

Figure 3. Lennard-Jones (12,6) approximation to the real intermolecular potential.

The other term included in the AIREBO model is the torsional potential, E_{kijl}^{tors}, which is the energy contribution from the rotation of the outer atomic bonds on a dihedral angle. It is an important contribution because its low internal rotation barriers can result in changes in the conformation of the molecule.

The torsional energy function is also periodical because of the possible 360° rotation for a given dihedral angle. This periodicity means that the torsional potential can be approached as a series expansion in relation to the torsional angle:[10]

$$E_{kijl}^{tors}(\omega) = \sum_n V_n \cos\,(n\omega) \qquad \text{(Eq. 9)}$$

The more terms included in the potential calculation, the more accurate it will be. Normally, a three-term approximation is used, see Figure 4 for the representation of each term in relation to the real one. The dotted line in Figure 4 serves as a baseline to measure the resulting potential for each approximation.

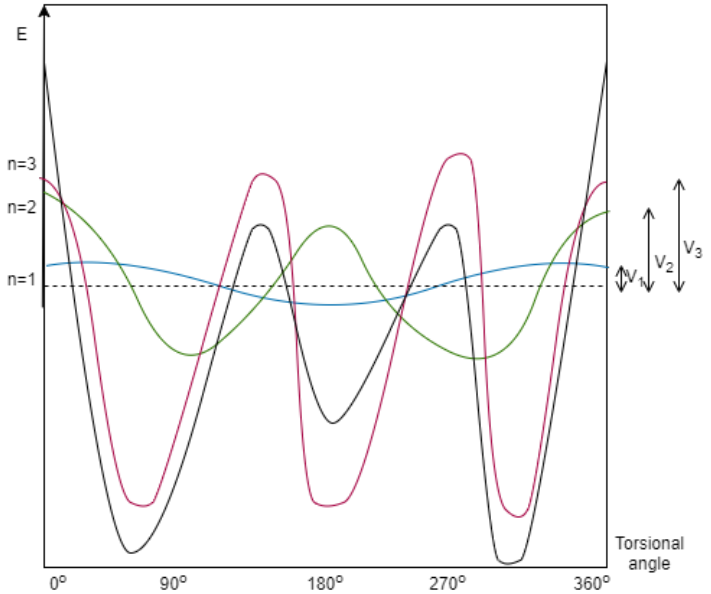

Figure 4. Three first terms of the torsional potential series expansion (colored) and the real torsional potential (in black).

As seen, the AIREBO potential aims to offer a more accurate approach to interatomic interactions by refining the REBO potential and including the summation of the (12,6) Lennard-Jones and torsional potentials.

5.3 MEMBRANES

Membranes are thin, porous layers of a material acting as a selective barrier for the effective separation of components in a mixture. While there are many different origins for membranes,

such as the biological ones, present in human cells, tissues and more, the focus of this study is in gas separation performed with carbon-based synthetic membranes.

The process of gas separation usually follows the diagram shown in Figure 5, in which a gas feed flows through a chamber in which a membrane is placed and is then separated into permeate (the molecules that passed through the membrane) and retentate (the molecules that were unable to be filtered). Both fractions can be obtained as isolated products if the separation is effective.

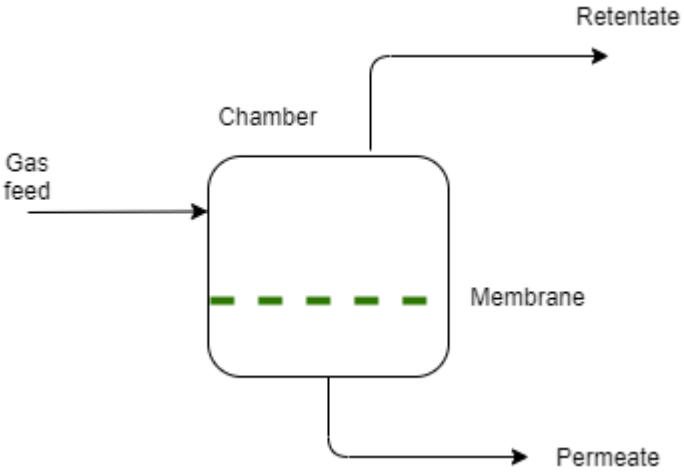

Figure 1. Diagram for a general gas separation process with a membrane.

The driving force for gas separation is the diffusion of the molecules through the pores of the membrane. Molecules that can permeate are expected to flow from a highly concentrated region to one of lower concentration. The rate of this process depends on temperature, pressure, size, and interaction between molecules, as explained above, as well as selectivity and permeability of the membrane.

5.3.1 Selectivity, Permeability and Permeance

Given a gaseous mixture of compounds A and B, the selectivity of a for compound A over compound B can be calculated as a simple ratio, the selectivity of the membrane was calculated using the following (Eq. 6) general equation for A over B on a gaseous mixture:[11]

$$S_{A/B} = \frac{x_A/x_B}{y_A/y_B} = \frac{N_A/N_{0,A}}{N_B/N_{0,B}} \qquad \text{(Eq. 10)}$$

Where x and y are the mole fractions of each molecule group in the gaseous mixture and the other side of the membrane, respectively, for each component of the mixture and the N terms indicate the number of molecules. As the initial number of molecules is the same in this case, the calculations can be simplified in the following equation:

$$S_{A/B} = \frac{N_A}{N_B} \qquad \text{(Eq. 11)}$$

In order to characterize the permeability of the membrane, as grazynes are a theoretical one atom thick structure and permeability is linearly dependent of the gas flow, a quantitative approach to the molecular flow is calculated by the following equation:

$$F = \frac{N}{S \times T} \qquad \text{(Eq. 12)}$$

Where N is the number of moles of gas molecules that have passed through the membrane, S is the total surface area of the membrane (in m^2) and T is the running time of the simulation (in seconds).

Permeance is one of the two most important data values when characterizing a membrane, the other being the previously presented selectivity.[12] It was first defined as the volume of gas molecules which penetrate the membrane in a set amount of time under a pressure gradient[13], but it can be also explained by the number of gas moles[14], it can be further combined with the permeability formula (Eq. 7) to simplify the calculations see Eq.13.

$$p = \frac{N}{S \times T \times \Delta P} = F/\Delta P \qquad \text{(Eq. 13)}$$

Where N is the mole of gases permeating through the membrane, S is the surface area of the membrane, T is the running time of the simulation and ΔP is the pressure drop, which is considered to be 1 atm for all the pores. The permeance units are expressed in GPU (Gas Permeance Units), where 1 GPU amounts to 3.35 x 10^{-10} mol/m^2Pa.[15]

5.3.4 Kinetic Diameter

When studying MD simulations, one of the most important concepts in gas separation by membranes is size sieving, which means the permeation a molecule can perform on a membrane in relation to its dimensions. For this, different models have been used, mainly approaches concerning the Lennard-Jones approximation[16] and the widely accepted kinetic diameter.

The kinetic diameter approach proposes a way to measure the chance of a molecule colliding with another in relation to its electron cloud and is a preferred method to deal with the flaws in the LJ model.[17]

5.4. Grazynes

The valency of carbon allows its atoms to be arranged in different geometries, resulting in several variations in its structure and properties. Many carbon allotropes have already been discovered, since the classical diamond and graphite to recent families of nanocarbons, such as fullerenes and nanotubes, but many more are researched yearly.[18]

This research focuses on grazynes, which are a newly proposed family of 2D carbon allotropes consisting of graphene stripes linked to each other via acetylenic bonds. Graphene, in turn, is an atom-thick layer of graphite, exceling in its many properties such as being one of the strongest materials known,[19] presenting a great thermic and electric conductivity and being impermeable to every gas. This last property is the focus of this research, as the modification of linkages in grazyne can lead to defects in its net which would act as pores in the resulting membrane, meaning a different structures could be designed for the separation of different mixtures. See Figure 6 for two structure examples.

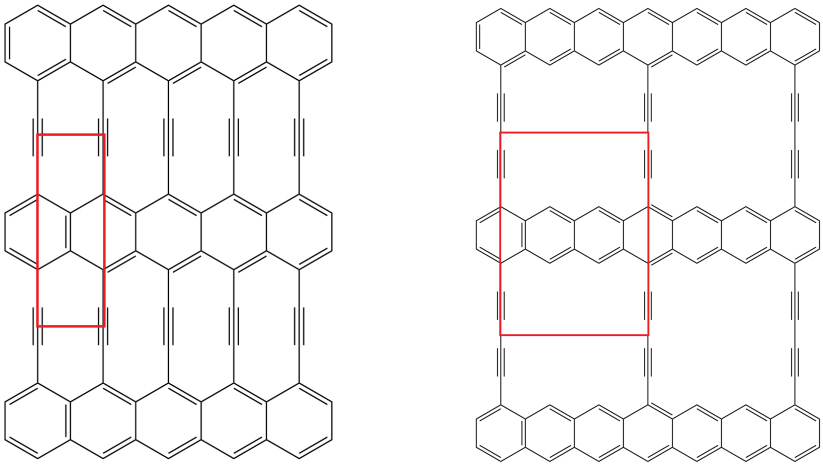

Figure 2. Sketches of the [1],[1]- and [1],[2]{2}-grazyne membranes (left and right, respectively), with their primitive cells underlined in red.

For graphene it is known that its properties can be reproduced periodically, meaning the properties seen in a unit cell can be reproduced in the next, it is expected that grazynes follow

the same periodical properties. The main interest in the grazyne family of allotropes comes from the size of the pores. Grazyne structures can vary in the number of acetylenic linkages between the graphene stripes, which confer a larger area where molecules could be filtered. The other way of modifying the pore area is by removing the acetylenic bond altogether, which is called the alternance and is performed periodically as seen for the [1],[2]{2}-grazyne structure in Figure 6.

Grazyne nomenclature follows the structure [n],[m]{p}-, where [n] is the number of graphene stripes, [m] is the number of acetylenic linkages and {p} is the number of graphene units without triple-bonded carbon atoms. Grazyne structures can also have more than one repeating unit cell, in which case (for example [1,2],[1]{0,1}-grazyne) but these structures were not considered for this research.

For the simulations, most low-pressure calculations (explained in the results section) have been performed with a supercell c(2x2). The supercell is not a different structure, it is a replication of the single cell to avoid overloading the system with many molecules and reduce computational constraints.

6. RESULTS AND DISCUSSION

6.1. Membrane Candidates Determination

The first step of this work was to design and visualize a couple of possible grazynic membrane candidates for the separation of a gaseous mixture. The CO_2/H_2O mixture was initially considered, but for reasons explained further below, it was finally decided to study CO_2/CH_4 and CO_2/O_2 mixtures. For the CO_2/H_2O separation, several primitive cells of grazyne membranes were designed.

The process of assembling a membrane is done via a coordinate file (.xyz). This file was edited manually and contains a header line with the number of atoms: 18 for both the [1],[3]-grazyne and the [1],[1]{1}-grazyne primitive cells (see Figure 1); and the spatial coordinates for every atom in the unit cell (in Ångström), preceded by its descriptor (C for carbon, H for hydrogen).

For the molecule geometry, the data from a previous research was used in order to obtain Carbon-Carbon bond distances[20] and the geometrical parameters were obtained from simple arithmetic calculations, see Table 1 for the distances.

	d(sp-sp)	*d(sp^2-sp)*	*d(sp^2-sp^2) x direction*	*d(sp^2-sp^2) y direction*
[1],[1]-grazyne	1.226	1.383	1.455	1.423
[2],[1]-grazyne	1.225	1.385	1.445	1.424
[3],[1]-grazyne	1.226	1.385	1.440	1.424

Table 1. C-C bond distances in Å for [n],[1]-grazyne (n=1,2,3)

For the present study, there were no interactions considered from the width of the benzenic strips, so the approximation to the optimized [1],[1]-grazyne bond distances was used. The membrane candidate was expected to follow the [1],[m]{p}-grazynes structure, because the length of the acetylenic linkage (represented here as m) and that linkage's alternance (here as p) are what defines the pore size.

To design the membranes, the main factors considered were the kinetic diameters of both CO_2 and H_2O molecules: 3.30 Å and 2.65 Å, respectively[21]. Knowing there is plenty of literature about the separation other molecules with similar kinetic diameter differences and high selectivity[22,23], membrane candidates were assembled so size sieving would be possible.

The suggested membranes were [1],[1]{1}-grazyne, with a pore area of 5.106 x 3.993 = 20.39 $Å^2$, and [1],[3]-grazyne, with a pore area of 2.553 x 10.294 = 26.28 $Å^2$. See Figure 1 for the unit cells. It is also worth mentioning that [1],[1]{1}-grazyne contains bonded hydrogen atoms in the

pore, but as they are able to move while attached to their respective carbon atom, the position of the hydrogen atoms is deemed variable and they are not considered when determining the pore length in the y-axis, as only an approximated range could be given.

[1],[3]-grazyne was chosen because its pore width (2.55 Å) was considered wide enough for the H_2O molecule to filter but not for the CO_2, based in the kinetic diameter of both molecules and possible steric repulsions. [1],[1]{1}-grazyne was selected because a recent study[24] shows that in [n],[1,2]{0,1}-grazynes (where n=1,2,3), CO_2 is filtered. It was decided that the [1],[1]{1}-grazyne contained a smaller pore area (shorter acetylenic chain) and was interesting to research if it was able to filter CO_2 and its selectivity with H_2O.

For the construction of the unit cells on the coordinates file, the bond distances at Table 1 were followed. As the cell was mainly linear, the position of most carbons depended only on the type of hybridization. The "central" benzenic atoms were trickier, but geometry calculations provided accurate values and both cells geometries were easily determined.

The lattice parameters were a = 5.11 Å and b = 6.81 Å for [1],[1]{1}-grazyne and a = 2.55 Å and b = 11.72 Å for [1],[3]-grazyne, while the c parameter was set at a very high value of 1500 Å to have enough empty space when performing pressure modifications, explained later on.

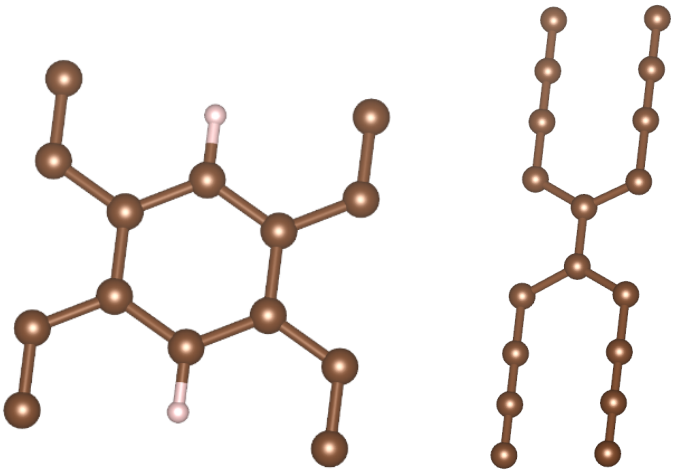

Figure 7. [1],[1]{1}- and [1],[3]-grazyne's primitive cells (left and right, respectively). Carbon atoms of the membranes are shown in brown while hydrogen atoms are represented in white.

Once the membrane's primitive cells were obtained, they were visualized via the Visualization for Electronic and Structural Analysis (VESTA) software, which offers a clear representation of the cells. See Figure 7 for the visualization of both membrane candidates. Later, Visual Molecular Dynamics (VMD) software was used because the software provides a cost-efficient depiction of the Molecular Dynamics simulation while offering a more schematical rendering.

Before starting to set the simulation's parameters, the two membrane candidates' unit cells were replicated using a Python script, to visualize them as a membrane and not as a unit cell.

The script would read the coordinates file, store each coordinate of an atom in a vector, and then save every atom as elements of a list. Then it would write a new file, assembling a 3x3 matrix which replicated the primitive cell by multiplying the coordinates of the atoms in the x- and y-axis. It would also need the lattice parameters set beforehand, as the coordinates file doesn't contain them. The script was also easily modifiable to change the matrix's dimensions, useful if the 3x3 matrix was not clear enough. It offered a firsthand approach to the membrane's geometry and reproducibility. See Figure 2.

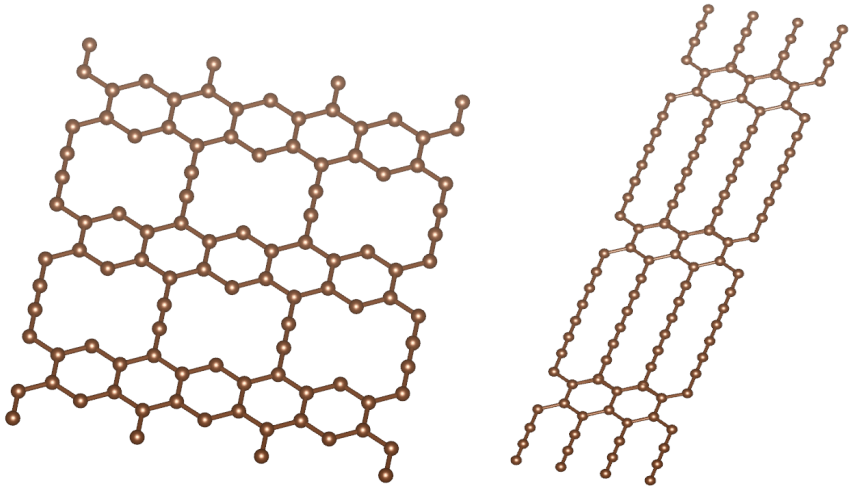

Figure 8. 3x3 matrixes of [1],[1]{1}-grazyne (left) and [1],[3]-grazyne (right), seen via VESTA.

It is worth noting that in Figure 8, hydrogen atoms for [1],[1]{1}-grazyne are not present. This is because of software limitations, but as the script was only used to obtain a preliminary visual representation it was considered alright for the general structure of the matrix. Later, the final input file was designed with the data of the primitive cell, as LAMMPS is able to replicate the cell

into a matrix of the desired dimension. Both hydrogen atoms and the mixture molecules were present in the final input file, which will be reviewed now.

6.2. Input File Design

Once the candidates for gaseous separation were developed, an input file was written with all necessary parameters and conditions for the LAMMPS simulation to be carried out. The input file consists of two text files containing the simulation parameters: the first one contains the geometrical and topological data and the second one the specific instructions for LAMMPS.

For the LAMMPS simulation to be performed, one of the important parameters to control are the size boundary limits of the simulation. This study is performed in a three-dimensional box where the total area of the membrane coincides with the box's width and length and a piston is set to control the pressure of the system. See Figure 9 for a snapshot of the system, where the simulation box can't be seen, but has been represented in the figure, because it's not a tangible item, but atoms can be appreciated confined in a region of space.

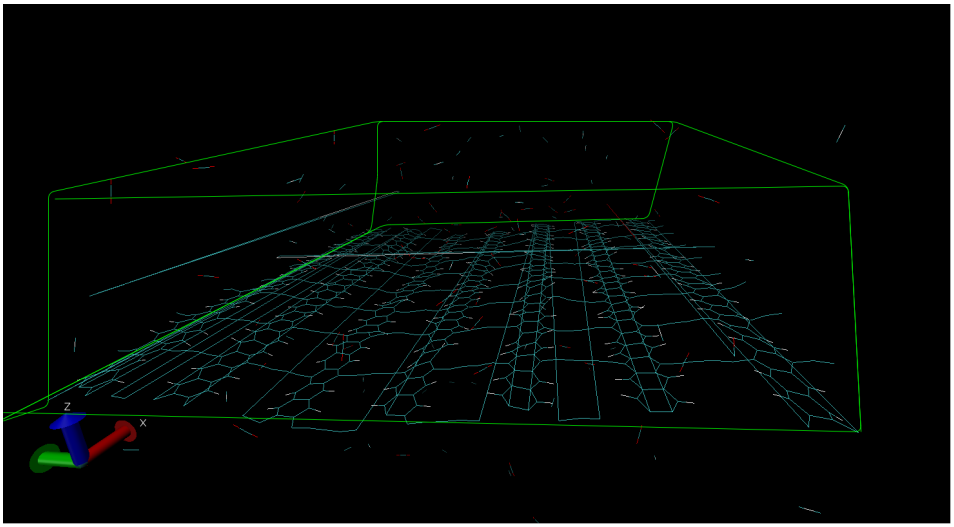

Figure 9. Snapshot of the [1],[2]{2}-grazyne membrane at 50 atm, gas molecules can be seen confined inside the simulation box (in green)

6.2.1 Data File

The data file contains the different information that allows to characterize each unit cell, while the replication conditions are set in the instructions file. The first group of data is the total number

of atoms, bonds, and angles per unit cell; then the type of each atom, bond and angle must be defined. Taking CH_4, for instance, there are 4 bonds in the molecule, but only one bond type.

After that, the unit cell parameters are introduced. As stated above, the c parameter, concerning the height of the cell, was set to 1500 Å because a piston would be used to simulate variable pressure values.

The next parameters are the definition of the atom types and the corresponding masses. Each atom type must be given a numerical descriptor and its mass value. It is worth noting that when considering the O_2 molecule, the data file needs to contain a new atom group which is a dummy. That's because angles are defined by 3 atoms and then an X atom with almost no mass is set between the two oxygen atoms. As the simulations pretend to offer an accurate approach to the real system, the addition of a dummy is a better solution than not defining the angle (and its associated energy).

The next step is the input of the coordinates and the electric charge for each atom of the unit cell, while defining the molecules (here as groups). Each atom is defined in a line of the following style, but separated only by a space:

```
Atom_index|group|atom_type|charge|x_coord|y_coord|z_coord
```

The final steps are the definition of the bonds and angles, which are set in the following way, again separated only by a keyboard space:

```
bond index|bond type|atom index 1|atom index 2
```

```
angle index|angle type|atom index 1|atom index 2|atom index 3
```

Where the energies, lengths and degrees were defined in the instructions file.

6.2.2 Input File

This is the main file for the LAMMPS software to perform the simulation, it contains all the energetic parameters not defined in the data file and the conditions for the study.

The file header are the basic settings used:

- *units metal*: this command defines the units used for the simulation. In this case, metal units mean Å for distance, picoseconds (ps) for time, eV for energy, Kelvin (K) for temperature and bars for pressure.
- *boundary p p p*: this command sets the periodicity for every lattice parameter. The p p p style means that the simulation box is periodical in all three axes.

- *dimension 3*: self-explanatory, it means it is a 3D simulation.
- *atom_style full*: this command sets the atomic attributes that will be considered during the simulation. full means that atoms will be treated as point particles and will be considered as molecules with charge.

After that the force field and the system conditions are introduced, starting with the type of representation for bonds and angles (harmonic, in this case, as explained in the theory section) and the instruction to read from the data file.

For the energetic calculations, mass and charge values must be introduced again before setting the force field. The force field is set via the *pair_style* command, in which it was an AIREBO potential, with a cutoff value of 2.5 Å for the LJ term and both torsional and LJ terms were considered for the force field. The simulation also used a further hybrid AIREBO/LJ potential, this is because only hydrocarbon atoms interact via the AIREBO potential, while the other interactions are calculated with the LJ one.

The next step was to set the pairwise force field coefficients for each pair of atom types. This is done with the *pair_coeff*. For the membrane atoms it is easy as the AIREBO model already does it. For the atoms not modelled by the AIREBO potential, each pairwise interaction must have the applied force field defined. In this case the interactions were defined as *lj/cut/coul/long*, which means the standard LJ 12,6 potential while also considering coulombic interactions and the long-range model. Cutoff values (in Å) must be introduced for LJ and coulombic interactions. This was considered a critical step for the initial mixture (CO_2/H_2O) because the cutoff values need to be obtained via bibliographical research and its search was considered beyond the time scope of the project. Thus, the final studied mixtures were decided to be CH_4/CO_2 and O_2/CO_2, as stated at the beginning of the results section, because the research group had already obtained data for their LAMMPS simulations.

To continue, the matrix dimension is defined via the *replicate* command and the atom types are set as molecules using the *group* command. The groups g_C, g_O2 and g_CO2 were set. With g_C for C and H atoms in the membrane and g_O2 for O atoms but also the dummy. Furthermore, a *fixed* group was created for a carbon atom to fix the membrane in space so to avoid the membrane from breaking apart. A *molec* group was also created to group the gaseous molecules (O_2 and CO_2). After that the *group subtract* style is used to group all molecules except

the O_2 and the fixed carbon atom in a new group (here called *MD*) to later set the thermodynamic conditions.

Later, the *kspace_style* command was used to apply a solver for long-range Coulombic interactions to be used for each timestep. In this case the *pppm* style was used, which solves a 3D mesh containing the atoms' charge.[25] For a large system it is preferred over the traditional Ewald summation because the former scales exponentially while the *pppm* method scales logarithmically.[26]

Next, bond and angle coefficients were defined for each type by its energetic values and the distance (or angle) for them. Bond and angle coefficients also need arguments introduced, in this case the prefactor (K) and equilibrium value for distance (or angle), explained in the theory section, as they follow harmonic rules.

After that the *timestep* command is set, in this case to 0.0001, which means to calculate every 0.0001 ps. The *run* command, set to 4000000 means there were 400 picoseconds (4×10^{-10} seconds) of the simulated system calculated. A lengthier simulation time was only performed for CO_2/O_2, which simulated the system for 3 nanoseconds (3×10^{-9} seconds) with a 0.001 ps timestep. The CH_4/CO_2 mixture suffered from computational constraints because LAMMPS couldn't perform a lengthy simulation with the same timestep as the previous mixture, and keeping the 0.0001 ps timestep would mean a simulation running for almost a month, as the original one ran for three days. It was deemed unnecessary.

The created *MD* group is now invoked to apply the *velocity create* command, which in this case sets the molecules temperature to 300 K, applies a random number seed for different velocities to be applied on each processor, and sets the linear and angular momentum of the group of velocities to zero.

Finally, several fixes are applied for the simulation. The first fix is setting the piston-like wall which allows for working at defined pressure values. The walls, one set to control pressure and the other set to zero, are the vertical edges of the simulation box. The next fix is setting a thermostat for the *MD* group, in this case the ramp is 300 – 300, which means that the temperature is invariable. Then, the following fix treats the O_2 molecule as an independent rigid body and sets the same thermostat conditions as the *MD* group for it. Finally, the *fixed* group (the carbon atom whose movement is impeded) is invoked to use a *setforce 0 0 0* command which sets the forces the atom receives as zero in all three axes.

6.3. Molecular Dynamics Simulation

Before running the simulation, it was considered that the pore size of the pore for both membranes was not suitable for filtering the new gaseous mixtures. The pore size of [1],[1]{1}-grazyne was 5.106 x 3.993 Å, resulting on an area of 20.39 $Å^2$, and the pore size of [1],[3]-grazyne was 2.553 x 10.294 Å, with an area of 26.28 $Å^2$. The kinetic diameters of the components of both mixtures, CH_4, CO_2 and O_2, where 3.80, 3.30 and 3.46 Å, respectively.

For this reason, [1],[1]{1}- and [1],[3]-grazyne membranes were kept for a posterior study and a suggested membrane of [1],[2]{2}-grazyne, which had already been researched but no Molecular Dynamics studies had been performed yet. The pore size of this membrane is 7.668 x 5.588 Å, which results in an area of 42.85 $Å^2$. As seen in Figure 10, this membrane shows a broader unit cell than the proposed ones and middle-sized length for the acetylenic linkages.

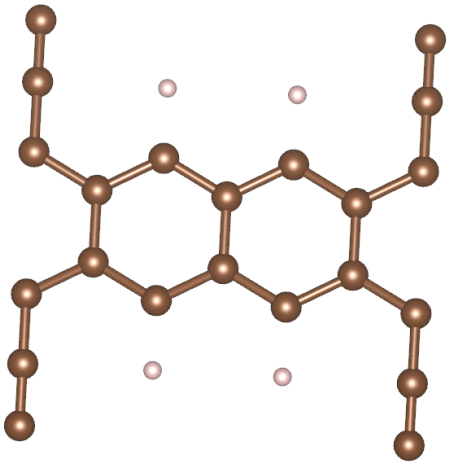

Figure 10. Primitive cell of [1],[2]{2}-grazyne.

6.3.1. Calculation of the Wall

As explained in the input file creation section, before the Molecular Dynamics study, to obtain the desired pressure values, a wall was simulated at different heights inside the box while the temperature remained constant at 300 K. Following the ideal gas law as an approximation and considering the box's dimensions, the piston-like wall was calculated to obtain an upper edge for every pressure value.

$$V = \frac{n}{N_A}\frac{RT}{P} \qquad \text{(Eq. 14)}$$

$$Z = \frac{V}{X \times Y} \qquad \text{(Eq. 15)}$$

Where X and Y correspond to the limit of the box in both respective axis and Z is the height at which the wall must be placed. Because the grazyne layer is always placed at a fixed height (70 Å), the final height of the wall is always shifted 70 Å higher than as calculated via Eq. 15. See Figure 11 for a diagram of the simulation box.

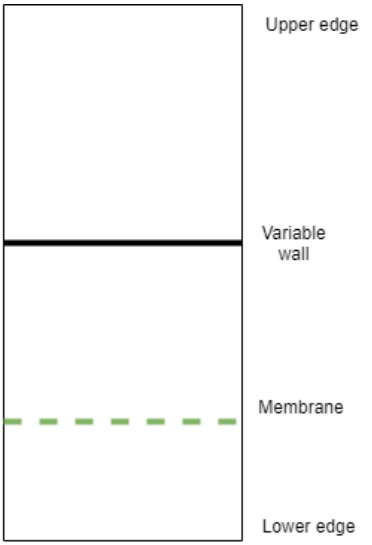

Figure 11. Diagram of the simulation box, the membrane is always set at 70 Å while the wall is variable.

Due to the height necessary to perform these simulations for low pressure values and the time of the simulation, it was considered that for studies at pressures lower than 10 atm (not included) a c(2x2) supercell had to be used in order to obtain a wider surface area while maintaining the same number of gaseous molecules, see Eq. 15. This was done because for higher wall values, the chance of the molecules reaching the membrane during the run time of the simulation would be significantly reduced.

Size of cell	P (atm)	V (Å^3)	z (Å)	z tot (Å)
c(2x2)	0,25	2.09 x 10^7	1128.7	1198.7
	0,5	1.05 x 10^7	564.4	634.4
	1	5.23 x 10^6	282.2	352.2
	2	2.61 x 10^6	141.1	211.1
	5	1.05 x 10^6	56.4	126.4
c(1x1)	10	5.23 x 10^5	112.9	182.9
	20	2.61 x 10^5	56.4	126.4
	50	1.05 x 10^5	22.6	92.6

Table 2. Wall height for different desired pressure values for both CO_2/CH_4 and CO_2/O_2 mixtures at 300 K.

The results for both mixtures are the same because the conditions of the simulation are identical and there is the same number of gas moles in each box.

6.3.2 LAMMPS Simulation

After the simulation conditions have been set in the input file, the file is submitted to LAMMPS to compute and the trajectory of the molecules is then evaluated. The LAMMPS simulation was set to print an output of the system's thermodynamical properties every 500 timesteps and the coordinates of each atom every 1000 timesteps, it was also set to perform 4,000,000 steps, which meant a simulated time of 0.4 ns (nanoseconds). The coordinates file shows the trajectory of the particles as a snapshot of every timestep, this allows for the study of the trajectory and the membrane's many properties. What is of most importance is how many molecules of each group trespass the membrane.

A Python script was designed to store the index of every molecule on a list if it appeared below the membrane, the value was set at 66 Å (4 Å below the membrane) to discard possible interactions performed when close to the layer. If the same molecule appeared at a value above 72 Å (2 Å above the membrane), it was considered that it permeated back to the original mix, then it would be removed from the list.

As every atom type was assigned an ID in the previously explained data file, the program would search every line for the IDs of CO_2, CH_4 or O_2 groups, compare them with the index of the stored atoms (to avoid repetition) and store them on one of the lists, one for each molecule.

To easily export the data to a spreadsheet, the script would write the timestep and how many atoms passed through the membrane for every timestep, using the following format:

```
Timestep_number | X_molecules_passed| Y_molecules_passed
```

Finally, to ease calculations concerning the final state of the system, the last line of the output file would print how many molecules of each type had permeated through the membrane in the following way:

"There have trespassed M molecules of X and N molecules of Y"

The output of the Python script was exported to a spreadsheet and then plotted in a permeated molecules vs timestep diagram. See Figure 12 for the performance of the membrane at 50 atm for the CO_2/CH_4 mixture as an example.

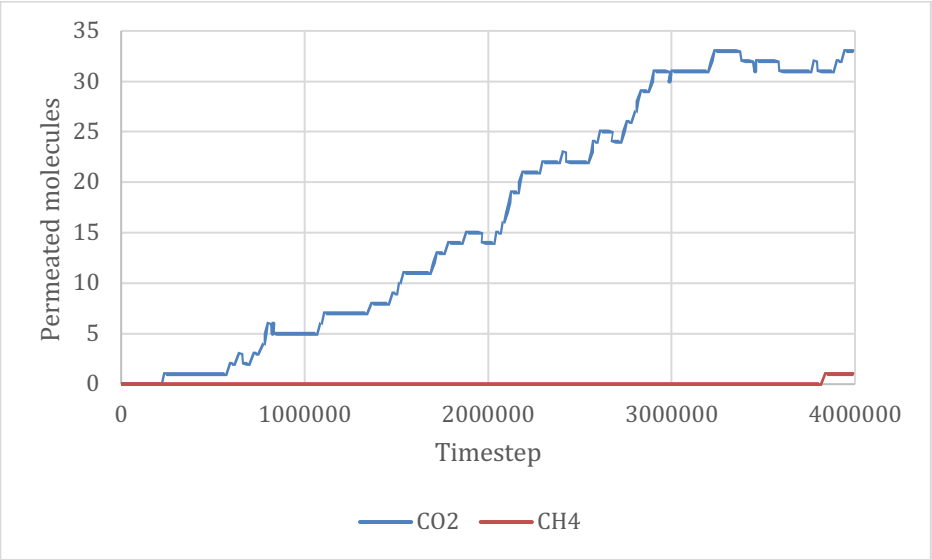

Figure 12. Number of permeating molecules for the [1][2]{2}-grazyne membrane at 50 atm and 300 K.

From the obtained plots it is seen that at a high enough pressure range (above 1 atm), gas permeation follows a linear dependence with time, so a linear regression could be performed to further study the simulation kinetics and other time-dependent parameters. Table 3 contains the number of molecules that passed through the membrane at the end of the simulation for each study.

	Mixture		Mixture	
Pressure (atm)	**CO_2**	**CH_4**	**CO_2**	**O_2**
0.25	0	0	0	1
0.5	0	0	2	1
1	4	0	0	1
2	14	0	8	3
5	22	0	10	13
10	11	0	5	8
20	19	0	10	16
50	33	1	19	25

Table 3. Number of gas molecules passing through the [1],[2]{2}-grazyne membrane at the range of 0.25 – 50 atm and 300 K.

Pressure (atm)	**$S_{CO2/CH4}$**	**$S_{O2/CO2}$**
0.25	-	∞
0.5	-	0.50
1	∞	∞
2	∞	0.38
5	∞	1.30
10	∞	1.60
20	∞	1.60
50	33.00	1.32

Table 4. Selectivity of CO_2 over CH_4 and O_2 over CO_2 molecules at the range of 0.25 – 50 atm and 300 K.

6.3.3 Study of Selectivity and Permeability

Using the value from Table 3, the membrane selectivity was calculated employing the method explained in Section 5.3.1. The selectivity values obtained are listed in Table 4. From the obtained selectivity values, it is clear that the membrane is a great separation method for the CO_2/CH_4 mixture, being infinitely selective at the pressure range of 1 – 20 atm and having a remarkable selectivity for high pressure values (i. e. over 20 atm). It is also worth noting that below 1 atm no molecules are filtered, a reason for this could be that to simulate a system below 1 atm, besides the use of the supercell c(2x2) which already means that there are less atoms per area, the wall is set so high (1198,7 Å for 0.25 atm, 634,4 Å for 0.5 atm) that the chance for the molecules to even reach the membrane during the simulated time (0,4 ns) is greatly reduced. The great difference in kinetic diameters, 3.80 Å for CH_4 and 3.30 Å for CO_2, and the obtained selectivity results indicate that size sieving is a notable way for the separation of CH_4 and CO_2 mixtures.

For the CO_2/O_2 mixture there is not enough data to determine if there is a preference of one molecule over the other, as for the pressure range from 0.25 to 2 atm the permeation seems arbitrary while for the 5 – 50 atm range the permeation of O_2 molecules seem slightly favored. Because both molecules are close in its kinetic diameter, 3.30 Å for CO_2 and 3.46 Å for O_2, size sieving with the [1],[2]{2}-grazyne membrane is not considered possible. Albeit that, a study was performed significantly extending the simulation time to 3 ns in order to consider if there is a possible equilibrium state in which selectivity could be better quantified. The results of Table 5 show that as time evolves, selectivity decreases and that the separation can be considered arbitrary due to the similarity in size for both molecules.

Pressure (atm)	n_{CO2}	n_{O2}	$S_{O2/CO2}$
0,25	2	0	0
0,5	3	5	1.67
1	7	10	1.43
2	24	20	0.83
5	34	29	0.85
10	25	27	1.08
20	33	37	1.12
50	50	52	1.04

Table 5. Number of permeating molecules and selectivity for the CO_2/O_2 mixture at the pressure range 0.25 - 50 atm, 300 K and 3 ns of simulation time.

Before determining that the [1],[2]{2}-grazyne membrane was not suitable for CO_2/O_2 separation, a final study was done at a set of temperatures to see if the membrane improved in performance at a certain temperature range. The chosen range was 200 – 600 K, with 100 K increments and it was performed at 1 and 10 atm to obtain a set of data for the supercell c(2x2) and for the normal cell membrane. The running time was set to the initial value of 0.4 ns.

Temperature (K)	n_{co2}	n_{o2}	$S_{O2/CO2}$
200	12	11	0.92
300	5	8	1.60
400	2	4	2.00
500	1	1	1.00
600	3	4	1.33

Table 6. Number of permeating molecules and selectivity for the CO_2/O_2 mixture at the temperature range 200 - 600 K and 10 atm.

Temperature (K)	n_{co2}	n_{o2}	$S_{O2/CO2}$
200	5	2	0.4
300	0	1	∞
400	0	1	∞
500	0	1	∞
600	0	2	∞

Table 7. Number of permeating molecules and selectivity for the CO_2/O_2 mixture at the temperature range 200 - 600 K and 1 atm.

Because of the small number of molecules filtered, it is determined that the results of Tables 6 and 7 again don't show conclusive data besides the randomness of the permeation preferences. It is also worth noting that to obtain higher temperature values, the upper wall had to be increased, as volume and temperature are linearly dependent of one another. That meant that there were less chances for the molecules to pass through the membrane during the running time.

All these results were convincing enough to determine that the [1],[2]{2}-grazyne membrane was not an efficient material for the filtering of the O_2/CO_2 mixture by size sieving separation.

Further studies were made to determine a capable membrane candidate for the separation of the O_2/CO_2 mixture. [1],[3]- and [1],[1]{1}-grazyne, the membranes initially designed for this work were profited as candidates because of their suitable pore areas. [1],[2]{1}- and [1],[3]{1}-grazyne membranes were also designed for working with a thinner pore than the [1],[2]{2}-grazyne but yet being of considerable size. See Table 8 for pore sizes and areas.

Membranes	**Pore size (Å)**	**Pore area (Å^2)**
[1],[3]-grazyne	2.55 x 10.29	26.28
[1],[1]{1}-grazyne	5.106 x 3.993	20.39
[1],[2]{1}-grazyne	5.106 x 5.588	28.53
[1],[3]{1}-grazyne	5.106 x 6.716	34.29

Table 8. Pore areas of the membrane candidates for CO_2/O_2 separation at 10 atm and 300 K

The simulation was performed at 10 atm and 300 K because it was the first pressure value at which the normal cell c(1x1) is used and 300 K is the temperature parameter at which all simulations were run. The simulation was also performed for a running time of 0.4 ns, same as the initial processes. All of the membrane candidates had a pore area smaller than the previous [1],[2]{2}-grazyne, that was because the intention of the candidates is to find a membrane capable of selectively separating one of the mixture's components. See Table 9 for the results.

Membranes	n_{co2}	n_{o2}	$S_{O2/CO2}$
[1],[3]-grazyne	0	0	-
[1],[1]{1}-grazyne	0	0	-
[1],[2]{1}-grazyne	0	0	-
[1],[3]{1}-grazyne	0	1	∞

Table 9. Number of permeating molecules and selectivity for the CO_2/O_2 mixture for different membranes at 300 K and 10 atm.

As the results in Table 9 showed that the [1],[3]{1}-grazyne could be infinitely selective for O_2 in the mixture, a further study was performed at 50 atm to check if a higher gas flow would confirm the selectivity of the membrane. The rest of the membrane candidates were not considered able to filter any of the gaseous molecules for 300 K and 10 atm because of their pore areas.

At 50 atm, the obtained results were of 2 O_2 and 1 CO_2 molecules filtered, which means a selectivity of 2.00 of O_2 over CO_2. The number of molecules is not large enough to be representative, but gives an approximation to the [1],[3]{1}-grazyne membrane as a better selective membrane for O_2/CO_2 separation than the previous [1],[2]{2}-grazyne membrane.

As explained in Section 5.3.2, an approximation to the permeability is performed with the gas flow. The obtained gas flow values are in the following table:

	Mixture		Mixture	
P (atm)	**F_{CO2}**	**F_{CH4}**	**F_{CO2}**	**F_{O2}**
0,25	0	0	0	22.71
0,5	0	0	45.42	22.71
1	89.43	0	0	22.71
2	313.00	0	181.70	68.14
5	491.86	0	227.12	295.26
10	983.73	0	454.25	726.80
20	1699.17	0	908.49	1453.59
50	2951.19	89.43	1726.14	2271.23

Table 10. Gas flow values (in mol/m^{2}s) for both gaseous mixtures and separated CO_2 and O_2 values for the O_2/CO_2 mixture.

For the permeability study it was important to determine the permeability of the individual components of both mixtures. As methane was considered to not be filtered, the only obtained value for its gas flow was deemed negligible. It is interesting that CO_2 shows a higher flow for the CO_2/CH_4 mixture than for the CO_2/O_2 one (see Figure 13). That is because in the CO_2/CH_4 mixture all the permeation is realized by CO_2 while in the CO_2/O_2 both molecules are able to permeate and the number of total molecules at the other side of the membrane increases faster. This means

that the rate at which CO_2 pass through the membrane in the CO_2/O_2 is slower because the gas flow is a summation of every gas molecule passing.

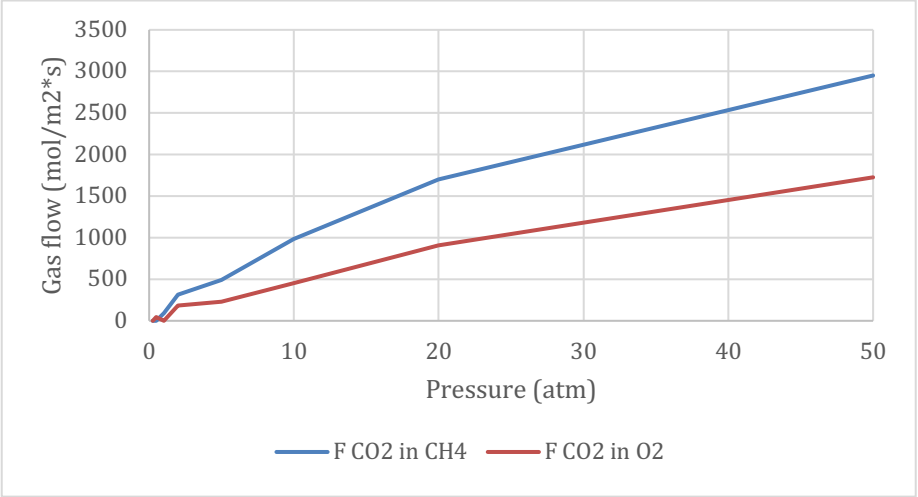

Figure 13. Gas flow of CO_2 with CH_4 and CO_2 with O_2 for the pressure range 0.25 – 50 atm and 300 K for the [1],[2]{2}-grazyne membrane.

The obtained results show a higher flow for O_2 instead of CO_2. Even though O_2 has a larger kinetic diameter (3.46 vs 3.30 Å), the molecule presents a shorter length (bond distance-wise) and CO_2 presents a higher adsorption energy on graphene[27], which could be the reasons for this phenomenon. See Figure 14.

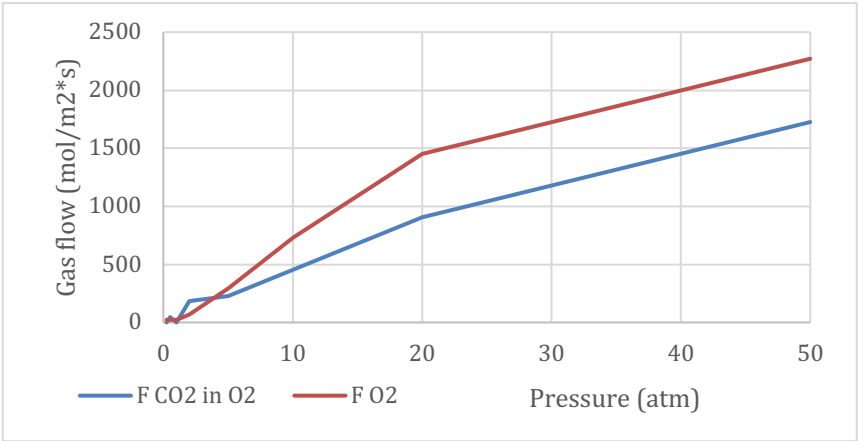

Figure 14. Gas flow of CO_2 and O_2 molecules for an increasing pressure in the [1],[2]{2}-grazyne membrane for permeability study.

As expected in both mixtures, the number of molecules permeating through the membrane increased with higher pressure values. The use of a supercell c(2x2) doesn't seem to influence permeability as the gas flow trend follows a linear behavior.

6.3.4 Study of Permeance

As explained in Section 5.3.3, permeance was calculated as the gas flow divided by the pressure drop, which was considered 1 atm, and then converted to GPU, see Table 11.

	Mixture		Mixture	
P (atm)	p CO_2	p CH_4	p CO_2	p O_2
0,25	0.00	0.00	0.00	6.59×10^5
0,5	0.00	0.00	1.34×10^6	6.69×10^5
1	2.64×10^6	0.00	0.00	6.69×10^5
2	9.22×10^6	0.00	5.5×10^6	2.01×10^6
5	1.45×10^7	0.00	6.69×10^6	8.70×10^6
10	2.90×10^7	0.00	1.34×10^7	2.14×10^6
20	5.01×10^7	0.00	2.68×10^7	4.28×10^7
50	8.69×10^7	2.64×10^6	5.09×10^7	6.69×10^7

Table 11. Permeance values in GPU of the [1],[2]{2}-grazyne for all components of both gaseous mixtures.

For the obtained values it is seen that gas permeance increases with the system's pressure on a linear basis. For the CO_2/CH_4 mixture not much can be said because the membrane's permeance for methane is almost negligible, as only one CH_4 molecule was able to permeate during the running time of the simulation, and only when simulated at 50 atm. For CO_2 in CO_2/CH_4, the same as in the other calculations can be said, as CO_2 permeance in this membrane is the only contribution to its permeation. The obtained permeance values correspond with the expected ones in other graphene-like membranes (in the range of 10^7 GPU) for CO_2, see Table 12, while not enough data is available to determine methane's permeance.

Membrane	[1],[2]{2}-grazyne	GDY-H[14]	Graphenylene-1[28]	γ-GYN[29]	g-C_2O[30]
Pressure (atm)	2	3	3	1	7.8
Permeance (GPU)	9.22 x 10^6	1.06 x 10^8	2.6 x 10^7	1.5 x 10^7	9.4 x 10^6

Table 12. Permeance values for CO_2 in different membranes at similar pressure values and 300 K.

Following the trends of the other analyzed parameters, permeance comparison for the CO_2/O_2 mixture shows higher values for the O_2 molecules, which was to be expected because permeance follows the same trend as permeability. Again, CO_2 permeance seems slightly favored for low pressure values but is steadily corrected since 2 atm. See Figure 15.

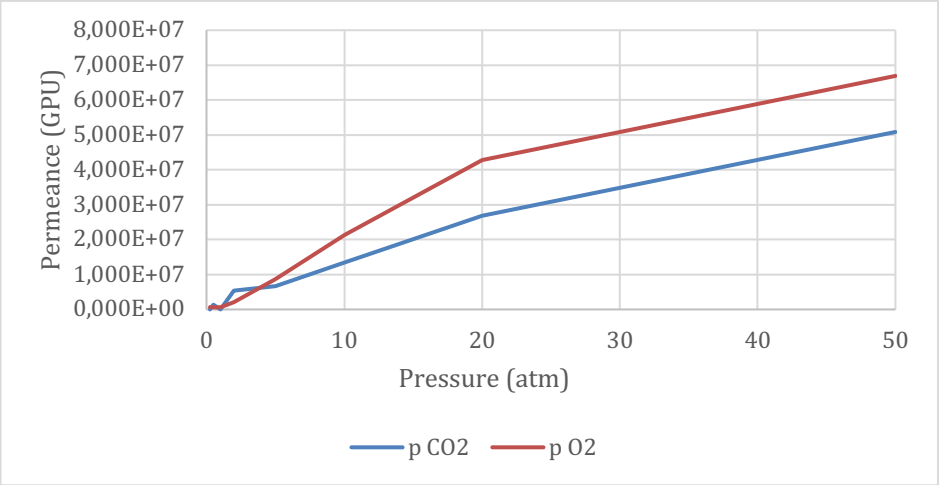

Figure 15. CO_2 and O_2 permeance (in GPU) of the [1],[2]{2}-grazyne at the pressure range of 0.25-50 atm.

A further study was performed for the permeance of CO_2 and O_2 at different temperatures and at 1 and 10 atm. From the results of Table 13 and the visualization of Figure 10, it is seen that the permeance of the CO_2 and O_2 molecules traversing the membrane is linearly diminished as temperature increases.

	1 atm		10 atm	
T (K)	**P CO_2**	**P O_2**	**P CO_2**	**P O_2**
200	1.34 x 10^7	5.35 x 10^6	3.21 x 10^7	2.94 x 10^7
300	0	2.68 x 10^6	1.34 x 10^7	2.14 x 10^7
400	0	2.68 x 10^6	5.35 x 10^6	1.07 x 10^7
500	0	2.68 x 10^6	2.68 x 10^6	2.68 x 10^6
600	0	5.35 x 10^6	8.03 x 10^6	1.07 x 10^7

Table 13. Permeance values in GPU for the CO_2/O_2 mixture at a 200 – 600 K temperature range and 1 and 10 atm for the [1],[2]{2}-grazyne membrane.

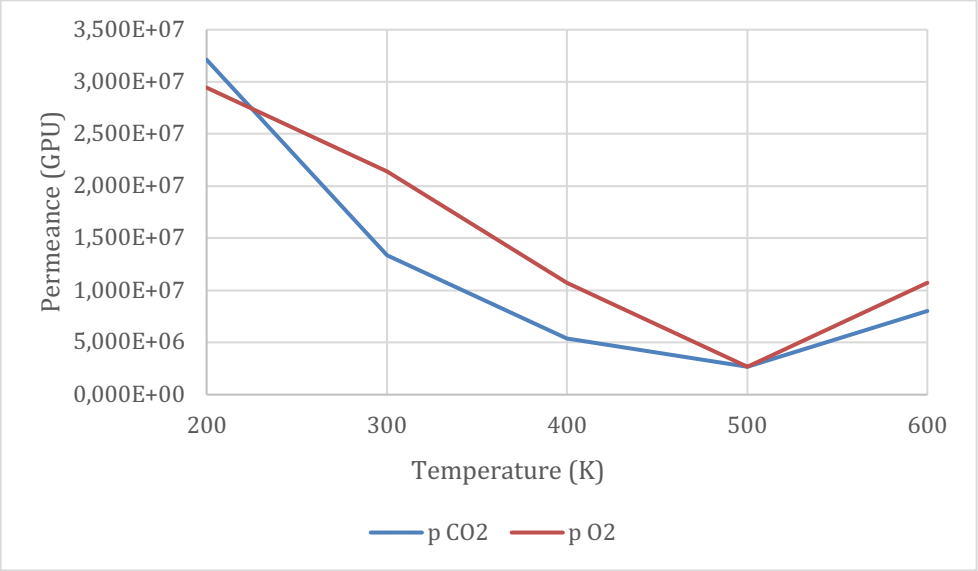

Figure 10. CO_2 and O_2 permeance (in GPU) of the [1],[2]{2}-grazyne at the temperature range of 200 – 600 K and 10 atm.

As only one molecule penetrated the membrane for each temperature set at 1 atm, the resulting data was not enough to perform an analysis. This and the decay in permeance for the 10 atm simulation are caused by the simulation box parameters. As the temperature was gradually increased for each simulation, it is directly correlated to the height of the simulation box. For relatively short running times, the chances for molecules to traverse the simulation box

and reach the membrane are greatly decreased. It is also seen that while the box is larger for higher temperature values, an exception occurs for 600 K, where permeance increases. This can be explained because the velocity gained by the particles is high enough to cover more distance during the simulation time.

7. CONCLUSIONS

From the obtained data treatment of the simulations, several conclusions can be extracted:

- The [1],[2]{2}-grazyne membrane is an infinitely selective membrane for CO_2 over CH_4 in the pressure range of 1 – 20 atm and 300 K, independently of the c(2x2) supercell or the c(1x1) cell. Above 20 atm the selectivity is high enough to be considered highly selective. Below 1 atm no molecules of the CO_2/CH_4 mixture are filtered.
- The [1],[2]{2}-grazyne membrane is found to not be selective for the CO_2/O_2 mixture for any pressure range. Neither are most of the other candidates, with the [1],[3]{1}-grazyne showing promising results but needing a larger simulation time to obtain conclusive data.
- The gas flow, which is used to obtain an approach to permeability, shows a significantly higher permeability for CO_2 in the mixture with CH_4 than in the mixture with O_2. This preference means diffusion rates are increased when only one molecule contributes to diffusion as the concentration of both sides must reach an equilibrium.
- From the simulation performed using a larger integration time (3 ns), it is seen that permeation through the membrane is higher during the first half of the simulation, confirming the driving force for the separation is the concentration gradient, which decreases as molecules permeate.
- The comparation of CO_2 permeance with other researched membranes shows slightly lower values for the [1],[2]{2}-grazyne membrane, this is to be expected when considering the CO_2/CH_4 mixture because as selectivity increases, permeance usually decreases, in compliance with the expected Robeson limit.

Summarizing the obtained results, it can be said that [1],[2]{2}-grazyne is an efficient membrane for the separation of CO_2 over CH_4 without sacrificing much permeance values and that [1],[3]{1}-grazyne might offer a decent method for the separation of O_2 in CO_2, but further research is needed.

8. REFERENCES AND NOTES

1. United Nations. Department of Economic and Social Affairs: Transforming our world: the 2030 Agenda for Sustainable Development. https://sdgs.un.org/2030agenda (accessed May 10, 2021)
2. Membrane Separation. Baker, R. Encyclopedia of Separation Science, 1st ed.; Academic Press, 2000; Vol. 1, pp 189-210.
3. Frenkel, D.; Smit, B. *Understanding Molecular Simulations*, 2nd ed.; Academic Press, 2001; Vol. 1, p 63
4. Introduction to Molecular Dynamics Simulation. Allen, M. P. Computational Soft Matter: From Synthetic Polymers to Proteins, Lecture Notes, 1st ed.; NIC Series, 2004; Vol. 23, pp 1-28.
5. Swope, W., Andersen, H., Berens, P., & Wilson, K. A Computer Simulation Method for the Calculation of Equilibrium Constants for the Formation of Physical Clusters of Molecules. J. Chem. Phys. **1982**, 1, 637-649.
6. Harrison, J. et al. Review of Force Fields and Intermolecular Potentials Used in Atomistic Computational Materials Research. Appl. Phys. Rev. **2018**, 3, 031104.
7. Tersoff, J. New Empirical Approach for the Structure and Energy of Covalent Systems. Phys. Rev. B. **1988,** 12, 6991-7000.
8. Stuart, S.; Tutein, A.; Harrison, J. A Reactive Potential for Hydrocarbons with Intermolecular Interactions. J. Chem. Phys. **2000**, 14, 6472-6486.
9. Atkins, P.; de Paula, J. *Physical Chemistry for the Life Sciences*,1st ed.; W. H. Freeman: New York, 2006; pp 469-472
10. Computational Chemistry. Hofmann, M.; Schaefer, H. Encyclopedia of Physical Science and Technology, 3rd ed.; Academic Press, 2003; pp 487-506.
11. Wall, Y.; Braun, G.; Kaltenborn, N.; Voigt, I.; Brunner, G. Separation of CO_2/N_2 by Means of a Carbon Membrane. Chem. Eng. Technol. **2012**, 3, 508-512.
12. Tabe-Mohammadi, A. A Review of the Applications of Membrane Separation Technology in Natural Gas Treatment. Sep. Sci. Technol. **1999**, 10, 2095-2111.
13. Transportation, Processing, and Refining Operations. Khan, M.; Islam, M. The Petroleum Engineering Handbook: Sustainable Operations, 1st ed.; Gulf Publishing, 2008, pp 295-364.
14. Rezaee, P.; Naeij, H. A New Approach to Separate Hydrogen from Carbon Dioxide using Graphdiyne-Like Membrane. Sci. Rep. **2020**, 1, 13549.
15. Liu, H.; Dai, S.; Jiang, D. Insights into CO_2/N_2 Separation Through Nanoporous Graphene from Molecular Dynamics. Nanoscale, **2013**, 20, 9984.
16. Breck, D. W. Zeolite Molecular Sieves: Structure, Chemistry and Use. John Wiley & Sons: New York, 1974
17. Transport of Gases and Vapors in Glassy and Rubbery Polymers. Matteucci, S.; Yampolskii, Y.; Freeman, B. D.; Pinnau, I. Materials Science of Membranes for Gas and Vapor Separation; Wiley: New York, 2006; pp 1−47.
18. Hoffmann, R.; Kabanov, A.; Golov, A.; Proserpio, D. Homo Citans and Carbon Allotropes: For an Ethics of Citation. Angew. Chem. Int. Ed. Engl. **2016**, 37, 10962-10976.
19. Wang, Z. et al. Review of Borophene and its Potential Applications. Front. Phys. **2019**, 3, 33403
20. Kamalinahad, S.; Viñes, F.; Gamallo, P. Grazynes: Carbon-Based Two-Dimensional Composites with Anisotropic Properties. J. Phys. Chem. C. **2019**, 44, 27140-27149.
21. Ismail, A.; Khulbe, K.; Matsuura, T. *Gas Separation Membranes*, 1st ed.; Springer, 2015, p 14
22. Zhang, Y. et al. Current Status and Development of Membranes for CO_2/CH_4 Separation: A Review. Int. J. Greenh. Gas Control. **2013**, 12, 84-107.
23. Lei, L. et al. Preparation of Carbon Molecular Sieve Membranes with Remarkable CO_2/CH_4 Selectivity for High-Pressure Natural Gas Sweetening. J. Membr. Sci. **2020**, 614, 118529.
24. Calzada, A. TFG research, Universitat de Barcelona, 2021.

25. Pollock, E.; Glosli, J. Comments on P_3M, FMM, and the Ewald Method for Large Periodic Coulombic Systems. Comput. Phys. Commun. **1996**, 2-3, 93-110.
26. Hockney, R.; Eastwood, J. *Computer Simulation Using Particles*, 1st ed.; CRC Press: Bristol, 1988.
27. Wu, H. et al. Adsorption of H_2O, H_2, O_2, CO, NO and CO_2 on graphene/g-C_3N_4 nanocomposite investigated by density functional theory. Appl. Surf. Sci. **2020**, 614, 118529.
28. Rezaee, P; Naeij, H. Graphenylene–1 Membrane: An Excellent Candidate for Hydrogen Purification and Helium Separation. Carbon. **2020**, 157, 779-787.
29. Sang, P. et al. Excellent Membranes for Hydrogen Purification: Dumbbell-Shaped Porous γ-Graphynes. Int. J. Hydrog. Energy. **2017**, 8, 5168-5176.
30. Zhu, L. et al. Theoretical Study of H_2 Separation Performance of Two-Dimensional Graphitic Carbon Oxide Membrane. Int. J. Hydrog. Energy. **2017**, 18, 13120-13126.

9. ACRONYMS

MD: Molecular Dynamics

LAMMPS: Large-scale Atomic/Molecular Massively Parallel Simulator

AIREBO: Adaptive Intermolecular Reactive Empirical Bond Order

VESTA: Visualization for Electronic Structural Analysis

VMD: Visual Molecular Dynamics

LJ: Lennard-Jones

MC: Monte Carlo

PBC: Periodic Boundary Conditions